*Archaeometry* **48**, 1 (2006) 97–114. Printed in Singapore

# DISTINCT, LATE BRONZE AGE (*c*. 1650 BC) WALL-PAINTINGS FROM AKROTIRI, THERA, COMPRISING ADVANCED GEOMETRICAL PATTERNS*

C. PAPAODYSSEUS,† TH. PANAGOPOULOS, M. EXARHOS,
D. FRAGOULIS, G. ROUSSOPOULOS, P. ROUSOPOULOS,
G. GALANOPOULOS and C. TRIANTAFILLOU

*National Technical University of Athens, School of Electrical and Computer Engineering, 9 Heroon Polytechneiou, GR-15773, Athens, Greece*

and A. VLACHOPOULOS and C. DOUMAS

*National University of Athens, Akrotiri Excavations, Thera, Greece*

*This paper studies a set of wall-paintings of the Late Bronze Age (*c. *1650 BC) initially decorating the internal walls of the third floor of the edifice called 'Xeste 3', excavated at Akrotiri, Thera, whose restoration is now in progress. It deals with the methods used for the drawing of the geometrical figures appearing in these wall-paintings. It is demonstrated that most of the depicted configurations correspond with accuracy to geometrical prototypes such as linear spirals and canonical polygons. It is pointed out that the steady lines of the figures, their remarkable repeatability, the precision of the geometrical shapes and their even distribution in the wall-paintings indicate a very distinctive use of the 'Xeste 3' third floor, which is now investigated.*

*KEYWORDS:* AKROTIRI, THERA, AEGEAN SEA, BRONZE AGE WALL-PAINTINGS, PATTERN RECOGNITION, CURVE FITTING, ORIGINS OF GEOMETRY

## 1 INTRODUCTION

Akrotiri, on the Aegean sea island of Thera, is a Late Bronze Age settlement that flourished in the 17th century BC, a time that corresponds to the Late Cycladic I period. Extensive archaeological research over the past 35 years has shown that before the catastrophic eruption of the Thera volcano, in *c*. 1650 BC, Akrotiri suffered a major disaster due to earthquakes. After a short period, at the time when the inhabitants were repairing their houses, thick layers of volcanic ash covered the settlement and the entire island, ensuring the abundant preservation of buildings and artefacts. The population had probably escaped before the eruption and everything remained undisturbed in the ruined settlement until 1967, when Spyridon Marinatos began the excavation at the site.

Of all the finds unearthed at Akrotiri, the wall-paintings constitute the most significant contribution to our knowledge of Aegean art, civilization and society (Doumas 1990, 1992). The tremendous earthquake was the cause of the collapse of the underlying walls and wall-paintings,

*Received 10 November 2003; accepted 25 May 2005.
†Corresponding author: email cpapaod@cs.ntua.gr

but the succeeding eruption was the major factor in their excellent preservation. As a rule, the fragments of the murals have been preserved within the rooms that they originally decorated.

The excavations at Akrotiri have so far brought to light about 10 houses or larger edifices, of which only three have been fully explored. 'Xeste 3' is the conventional name for a free-standing edifice that lies in the southwestern part of the excavated settlement, close to where the quay and the port of the town are thought to have been. The building had 14 rooms on its ground floor and 14 on the second floor, but the central part was at least three storeys high. This monumental edifice, with impressive façades, a monumental staircase, a lustral basin and extensive use of pier-and-door partitions (*polythyra*) around it, has offered the largest assemblage of wall-paintings located to date at Akrotiri. Judging from the architectural peculiarities of the building and the themes of the wall-paintings, it may be concluded that 'Xeste 3' was a public building used for the performance of communal ritual activities. In this paper we will, for the first time, present and discuss a set of very important wall-paintings that initially decorated the internal walls of the third floor of 'Xeste 3'.

## 2 A GENERAL DESCRIPTION OF THE 'XESTE 3' THIRD-FLOOR WALL-PAINTINGS

This large composition from 'Xeste 3' depicts white–blue and red double spirals in pairs, forming symmetrical ivy-shaped motifs. This ensemble of wall-paintings was excavated in a highly fragmentary state. More than 5000 pieces belonging to it were found, ranging in size from few square millimetres to approximately 1 $m^2$, with an average of about 80 $cm^2$. The restoration of the composition is now in progress, and an original information system has been developed to assist the experts in this extremely difficult and time-consuming reconstruction process (Papaodysseus *et al.* 2002). The initial surface area of this wall-painting is unknown, but judging from the expansive dispersion and the quantity of the fragments, the painting might be larger than 40 $m^2$. This wall-painting was found in Rooms 3 and 4, and comes from the third floor of 'Xeste 3'. Since no blue and red spirals are depicted together on the fragments, we assume that these subjects decorated at least two different walls. The use of the relevant rooms of the third floor is not yet known, and we can only speculate about the original use of this section of the building, of which only scant architectural elements have survived.

The best-restored sections of this monumental wall-painting depict antithetical double spirals, each approximately 32 cm in diameter, with a black outline and dense red dots in between, along the stems. These pairs of spirals are depicted horizontally and create the upper decorative zone of the main composition, which comprises larger and more elaborated vertical pairs of double spirals that form colourful stylized ivy leaves. Rosettes with black petals in the middle of blue curvilinear lozenges, antithetical pairs of blue triangles outlined with elegant red crescents and other geometrical motifs evenly distributed on the composition complete the artistic vocabulary of this masterly wall-painting. The extensive use of incisions before the drawing of the spirals, the steady lines of the outlines, the almost identical dimensions of the spirals and their even distribution on the painted wall surface strongly indicate that the conception, development and execution of this huge geometrical subject were made according to a strict iconographic programme, which was adapted and adjusted to the architectural idiom of the third floor of 'Xeste 3'. In the subsequent sections of the present paper we will demonstrate that the accomplishment of this iconographical programme requires an advanced sense and application of geometry. To be more specific, all spirals belonging to this wall-painting theme follow a concrete geometrical prototype, while most decorative elements are placed along the radii of canonical polygons (mainly 48-gon, 32-gon or 16-gon).

## 3 A BRIEF HISTORY OF THE RELATED MATHEMATICS

In this section, we will give a brief description of knowledge in the Classical age mainly, in connection with the geometric configurations appearing in the considered wall-painting. In what follows, when a phrase of the type 'mathematician or philosopher X first stated and/or proved Proposition A' is used, this will mean that it is historically well founded that the statement or proof of Proposition A is onomastically attributed to person X. Indeed, the Greek mathematician Thales (Θαλής; 624–546 BC) seems to be the first to have stated that the circle is bisected by its diameter (Heath 1981 [1921], 130). Oinopides of Chios, in the fifth century BC, is so far considered, even by Proclus, to have been the first person to draw the perpendicular to a given straight line from a point outside it, using compasses. He is also so far considered to have been the first person to bisect a given angle.

Concerning spirals, the general mathematical definition is given in section 4. However, a non-strict general definition of a spiral can be given, as a kind of circle whose radius constantly increases with the corresponding angle. There are infinitely many types of spirals corresponding to the equally infinitely many ways in which the radius may be increased. So, for example, there is a type of spiral generated by unwrapping a thread around a peg, frequently called the involute of a circle. Another type of spiral, called logarithmic or exponential, is the one whose radius increases exponentially. We emphasize that both of these types of spiral can be encountered in nature. The involute of a circle can be easily generated in everyday life events, while the logarithmic spiral can be found in various cockleshells. Thus, it is not surprising that rough approximations of spirals—and, in particular, the types mentioned above—are encountered quite early in various prehistoric civilizations. On the other hand, the linear spiral referred to in the present paper, in which the radius increases linearly with the angle, seemingly does not exist in nature. Note that the columnar 3-D helix attested in the Old Babylonian civilization, frequently but erroneously called a 'linear spiral', has a completely different functional form and therefore has nothing to do with the linear spiral that appears in the considered Akrotiri wall-paintings (Robson 1999).

The mathematical definition of the linear spiral, which nowadays also bears Archimedes' name, is, so far, attributed to Conon (Κόνων) from Samos in the third century BC. In fact, Pappos (Πάππος) Alexandrinus, in his work 'Συναγωγή' ('Collection') in the fourth century AD, states that a theorem about the plane spiral was proposed by Conon and proved by Archimedes. Indeed, in 'On Spirals' Archimedes defines the linear spiral and gives its fundamental properties (Heath 1981 [1921], 230–1; Spandagos *et al.* 2000).

## 4 STRONG EVIDENCE THAT THE DEPICTED SPIRALS ARE LINEAR (ARCHIMEDES) ONES

As we have already pointed out, we have observed an impressive regularity in the spiral borders, which are drawn with a steady line, while the shape of the spirals manifests remarkable repeatability. On the contrary, the contours of other drawings seem more irregular; as, for example, in the case of the black parallel lines on a cyan background (see Fig. 5 below), which are much easier to draw. In addition, the red dots appearing in the same figure to decorate the spirals seem more imperfect than the corresponding spirals themselves. The above observations imposed the idea that the artist, or artists (we will use the singular for convenience), almost 3700 years ago, used geometrical methods and/or handicraft stencils to draw the spirals. The scope of this section is to offer sufficient evidence to support the above assertion, as well as to give a plausible answer to the question concerning the method that the artist used to draw the spirals.

The developed methodology has been applied to images that have been taken under strict photographic conditions. More specifically, all photographs were taken indoors, with the same luminance conditions. It was ensured that both the camera and the fragment to be shot were horizontal. In addition, each fragment picture included scales, a triangular one with grids on it and a rectangular one with thematic chromatic pallets.

### *4.1 The general definition of a spiral*

It is well known that the general spiral equation is of the form

$$x(\theta) = x_0 + R(\theta) * \cos(\alpha(\theta)),$$

$$y(\theta) = y_0 + R(\theta) * \sin(\alpha(\theta)),$$

where $x_0$, $y_0$ is the centre of the spiral, $R(\theta)$ is any increasing function of $\theta$ and $\alpha(\theta)$ is any function of $\theta$. Amongst the various spirals, the most celebrated ones are the following:
(1) The Archimedes spiral; namely, the one with $R(\theta) = k * \theta$ and $\alpha(\theta) = \theta - \phi_0$, where $k$ is a constant, while $\phi_0$ accounts for a probable rotation of the spiral.
(2) The spiral that corresponds to unwrapping a thread around a nail, stake or peg, which is frequently called the 'involute of a circle', with $R(\theta) = r_0\sqrt{1 + \theta^2}$ and $a(\theta) = \theta - \arctan(\theta) - \phi_0$, where $r_0$ is a constant corresponding to the nail, stake or peg radius and, as before, $\phi_0$ accounts for a probable rotation of the spiral.
(3) The logarithmic spiral satisfying $R(\theta) = a * e^{\beta * \theta}$, $\alpha(\theta) = \theta - \phi_0$, where $\alpha$ and $\beta$ are constants and, once more, $\phi_0$ accounts for a probable rotation of the spiral.

### *4.2 Trying to match a wall-painting spiral to a specific equation*

We have extracted the boundaries of all spiral parts depicted in the available excavated fresco fragments. In this paper, with regard to the two boundaries of each spiral part, we have mainly chosen the one where the external to the spiral is locally convex, for demonstration purposes (see the corresponding computer-generated curve in Fig. 1). We will call this 'the internal boundary of the spiral'.

The scope is to find the theoretical model that best fits these painted spiral patterns, with the restriction that this model could have been generated by the artist using the means that we presume to have then been available. In order to do so, we have applied the following method.

We have considered each theoretical model to be a function of its parameters in the corresponding real multidimensional space. Thus, for example, we let the Archimedes, or linear, spiral be the pair of functions

$$x = x_0 + \kappa\theta\cos(\theta - \phi_0) = xL(x_0, \kappa, \phi_0),$$

$$y = y_0 + \kappa\theta\sin(\theta - \phi_0) = yL(y_0, \kappa, \phi_0).$$

In an analogous manner, the parameter space of the involute of a circle is $(x_0, y_0, r_0, \phi_0)$, while that of the logarithmic or exponential spiral is $(x_0, y_0, a, \beta, \phi_0)$.

Next, we have considered an arbitrary painted spiral pattern starting at a point B and ending at a point C, which we call the *actual spiral part*, or simply the *drawn spiral* (see the corresponding computer-generated line in Fig. 1). Moreover, we have let an arbitrary point $(x_0, y_0)$, coplanar to the spiral BC, be the hypothetical centre of the spiral theoretical model to which BC belongs. For an arbitrary theoretical model spiral, we connect the centre $M(x_0, y_0)$ with B

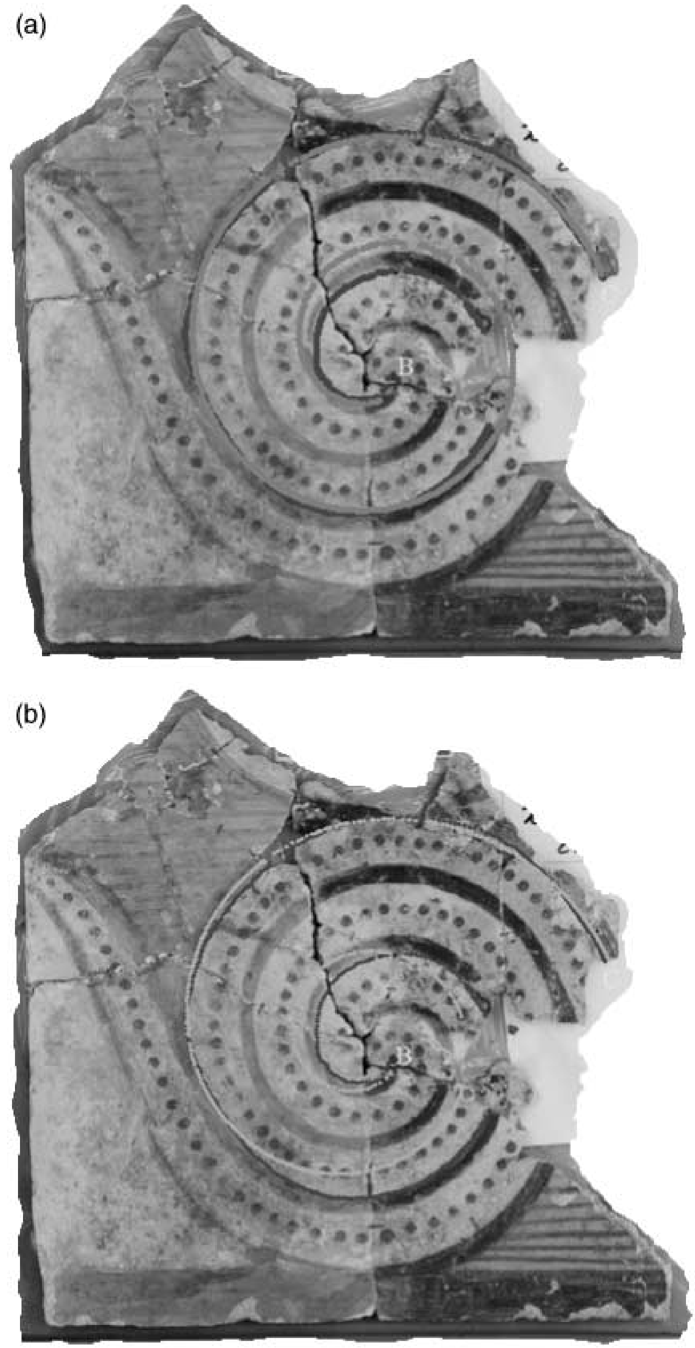


Figure 1 *(a) The way in which the theoretical model of the involute of the circle (the computer-generated light grey line) best fits to an actual spiral part (the computer-generated dark grey line). (b) The way in which the theoretical model of the logarithmic spiral (the computer-generated light grey line) best fits to an actual spiral part (the computer-generated dark grey line).*

and C and the centres of all intermediate pixels $(x_i^A, y_i^A)$ of BC, thus obtaining a set of radii corresponding to the actual spiral part:

$$R_i^A = \sqrt{(x_i^A - x_0)^2 + (y_i^A - y_0)^2}$$

Let $(x_i^M, y_i^M)$ be the point of the model spiral belonging to the line where $R_i^A$ also lies, nearest to $(x_i^A, y_i^A)$. Moreover, let $R_i^M$ be the distance of point $(x_i^M, y_i^M)$ from the model spiral centre $M(x_0, y_0)$. Subsequently, we have considered the error function $E$:

$$E^M(\text{model spiral parameter space}, \theta_B) = \sum_{i=1}^{N} \sqrt{(x_i^A - x_i^M)^2 + (y_i^A - y_i^M)^2},$$

where $N$ is the number of pixels of the drawn spiral part and $\theta_B$ is the angle that defines the point of the model spiral that corresponds to B.

Next, we have minimized the above-mentioned error function in its corresponding parameter space for three types of model spirals—the linear one, the exponential one and the involute of a circle—using a version of the conjugate gradient method as well as the Nelder–Mead method. Thus, we have obtained a set of parameters for each theoretical model that offers the best approximation of the drawn spiral part by the theoretical spiral in hand.

In fact, consider the actual spiral part depicted in Figures 1 and 2. The way in which each one of the three above-mentioned theoretical models best fits to this painted spiral part is shown in the figures: Figure 1 (a) for the involute of a circle, Figure 1 (b) for the exponential spiral and Figure 2 for the linear spiral, where both of the depicted spirals are approximated. From these figures it is evident that the linear spiral best approximates the considered spiral part of the specific wall-painting.


Figure 2 *The way in which the theoretical model of the linear spiral with k = 23.69 (the computer-generated light grey and dark grey lines) best fits to an actual pair of spirals.*

In the subsequent sections, we will offer essential evidence that all depicted spirals on the wall-paintings correspond to linear prototypes. In particular, we will prove that if the prototype model spirals are divided into a number of stencils, then an excellent approximation of all drawn spirals is achieved. In addition, we feel that it is necessary to eliminate the case that the spirals were drawn by means of unwrapping a thread, since this method of drawing does not necessitate an advanced sense and application of geometry. Note, however, that as $\theta \to \infty$, this spiral tends to the linear one. Thus, for example, for $\theta = 2\pi$ the difference between the two radii is 2.53%. Therefore, one must expect the difference between a linear spiral and the corresponding involute of a circle to be found in the initial part of the spirals.

### *4.3 Criteria for matching between a model spiral and an actually painted one*

Suppose that the artist wanted to draw a specific spiral model that is described in contemporary mathematics by the set of equations

$$x^M(\theta) = x_0 + R^M(\theta) * \cos(\alpha(\theta) - \phi_0),$$

$$y^M(\theta) = y_0 + R^M(\theta) * \sin(\alpha(\theta) - \phi_0).$$

Suppose, moreover, that the outcome of this effort is a spiral that, in a contemporary digital image, is actually a set of $N^A$ coplanar pixels (or equivalently, coplanar points) with coordinates $(x_i^A, y_i^A)$; namely, the set $\boldsymbol{S^A} = (x_i^A, y_i^A)$, $i = 1, \ldots, N^A$. After applying the analysis made in the previous section, it is possible to obtain the optimal position and parameters of the model spiral $\boldsymbol{S^M}$, so that it best fits the actual painted one $\boldsymbol{S^A}$. Hence, let the centre of this optimal model spiral $\boldsymbol{S^M}$ be $(x_{0,opt}, y_{0,opt})$ and let its radius function be $R^M_{opt}(\theta)$. Consequently, we have adopted the criterion shown below, which is a necessary condition for the matching of the actual and model spirals.

Consider, in the same plane, both the painted spiral $\boldsymbol{S^A}$, as well as the best fit to it, model spiral $\boldsymbol{S^M}$, placed in their best fitting positions. Moreover, consider the ensemble of straight semi-lines $\varepsilon_i$, $i = 1, \ldots, N^A$, starting at the centre $O(x_{0,opt}, y_{0,opt})$ of the model spiral, passing through the centre $A_i$ of all pixels of the actual painted spiral $\boldsymbol{S^A}$ and forming an angle $\theta_i$ with the $x$-axis (see Fig. 3 (a)). Suppose that the arbitrary semi-line $\varepsilon_i$ intersects the model spiral $\boldsymbol{S^M}$ at the point $M_i$, $i = 1, \ldots, N^A$, nearest to $A_i$. Clearly,

$$OM_i = R^M_{opt}(\theta_i), \quad i = 1, \ldots, N^A, \quad OA_i = R^A(\theta_i).$$

Next, we set the following quite general criterion:

CRITERION 1. *Suppose that the artist, probably by means of the use of an instrument or instruments, had the intention of drawing a (model) spiral* $\boldsymbol{S^M}$ *and that the result of his effort was the actual spiral* $\boldsymbol{S^A}$*. Then, the sequence* $\delta R_i$*, where*

$$\delta R_i = OA_i - OM_i = R^A(\theta_i) - R^M(\theta_i), \quad i = 1, \ldots, N^A,$$

*is a random variable coming from a population that has a zero mean value.*

It is quite evident that the above criterion constitutes a necessary condition for testing the probability that the artist had the intention of drawing a specific spiral model, but it is not a sufficient condition. In fact, relatively large symmetric fluctuations of the painted shape around the model spiral may satisfy Criterion 1. Therefore, a new criterion must be stated that

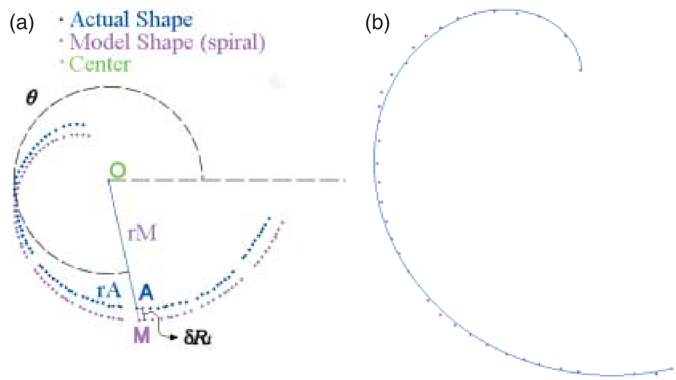


Figure 3 *(a) A demonstration of Criterion 1. This is an artificial figure, simply intended to display the parameters employed in Criterion 1: the details of an actual fit between a linear and a drawn spiral are depicted in Figure 3 (b). (b) A demonstration of the actual way in which the model spiral fits the real one.*

best describes the overall distance (fluctuation) of the actually painted shape from a model one. In fact, following Pearson *et al.* (1977), the quantity

$$S_P = \sum_{i=1}^{N^A} \frac{(R_i^M - R_i^A)^2}{R_i^M},$$

where $N^A$ is the number of drawn spiral points, follows a chi-square distribution with $N^A - n - 1$ degrees of freedom, where $n$ is the number of independent variables governing the model spiral equation. Thus, we define the following criterion of goodness of fit between a model and an actually painted spiral:

Criterion 2. *Consider the population size of the chi-square distribution with $N^A - n - 1$ degrees of freedom, lying at all points greater than $S_p$. We have the probability $P_s = P(x \geq S_P)$, which is the chosen measure of goodness of fit between spirals* $\boldsymbol{S^A}$ *and* $\boldsymbol{S^M}$.

*4.4 Rejecting the hypothesis that the artist drew the spirals by unwrapping a thread or rope around a stake or peg, by using Criterion 1*

Let us make the assumption that the artist drew the spirals by unwrapping a thread or rope around a stake or peg. It is, then, obvious from the previous analysis that the peg centre is at $O(x_{0,opt}, y_{0,opt})$, its radius is $r_0$ and that, in general, the model spiral $\boldsymbol{S^M}$ is placed in the position best fitting $\boldsymbol{S^A}$.

For example, consider the spiral depicted in Figure 1 (a), which consists of $N^A = 463$ points (pixels). The involute of a circle best fitting to it is defined by the parameters ($x_0 = 568.1$, $y_0 = 420.3$, $r_0 = 19.6$, $\varphi_0 = 0.1$).

At this point, we form the sequence

$$\delta R_i = OA_i - OM_i = R^A(\theta_i) - R^M(\theta_i), \quad i = 1, \ldots, N^A.$$

Before choosing it, we would like to point out that there are mainly two parameters influencing the exact form of the contour line of each spiral, which probably corresponds to a prototype stencil. The first parameter is associated with the stencil placement on the wall. The second parameter is related to the random deviations of the contour line from the prototype stencil, possibly due to a class of factors such as the relative instability of the artist's hand and/or slight, erratic movements of the paintbrush bristles and/or the fact that there may be no direct contact of the entire body of the stencil with the wet wall, and so on. Clearly, this class of factors is responsible for the random fluctuations of the drawn contour line from the corresponding stencil that the artist used as a guide to draw it. We feel that these factors may be considered to be stochastically independent in contour points differing by more than a small number of pixels. Hence, we choose a subsequence $\delta R_j$, $j = 1, 2, \ldots, M$, where two consecutive sequence elements $\delta R_j$, $\delta R_{j+1}$ correspond to neighbouring pixels of $\boldsymbol{S^A}$ having a separation of $d$ pixels, where $d$ is randomly chosen, with the restriction $5 \le d \le 8$. Application of the Kolmogorov test to the set $\delta R_j$, $j = 1, 2, \ldots, M$, confirms their stochastic independence.

Let $\bar{X}$ be the mean value and let $S^2$ be the variance of $\delta R_j$. Then, according to inductive statistics, the quantity

$$t = \frac{\bar{X}}{S/\sqrt{M}}$$

follows a Student distribution with $M - 1$ degrees of freedom. This quantity is computed for each of the available almost entire spirals, separately.

At this point we apply Criterion 1, in the sense that if the actually drawn spirals were involutes of a circle, then $\delta R_j$ comes from a population with mean value $\mu = 0$. Hence, we state the hypothesis $H_0 : \mu = 0$, against the hypothesis $H_1 : \mu \neq 0$, with confidence 99.9% or, equivalently, significance level $a = 0.001$, for all these spirals. According to inductive statistics, hypothesis $H_0$ is not rejected if $|t| \le t_H$, where the $t_H$ value depends on the degrees of freedom. Otherwise, hypothesis $H_0$ is rejected. Quantity $a$ expresses the probability that $H_0$ is indeed valid but that inequality $|t| > t_H$ holds. In the present case for the involute of a circle, $|t|$ ranges from 3.7 to 7.1, always satisfying $|t| > t_H$. Therefore, the obtained results indicate that the hypothesis that the depicted spirals were drawn by unwrapping a thread is rejected (see also Fig. 1 (a)).

In exactly the same way, the hypothesis that the depicted spirals correspond to logarithmic ones may be rejected (see also Fig. 1 (b)). Similarly, the hypothesis that the spirals have been drawn by using stencils that are pieces of an involute of a circle may be rejected. We must point out that the attempt of approximating the drawn spirals by parts of an involute of a circle fails in the first spiral revolutions, since the linear spiral and the one generated by unwrapping a thread around a peg asymptotically coincide as $\theta \to \infty$.

### *4.5 Confirming the hypothesis that the set of excavated spirals are linear spirals, by using Criterion 1*

Let us now make the assumption that the artist drew a linear spiral. Following the previous analysis, we consider spirals $\boldsymbol{S^A}$ and $\boldsymbol{S^M}$ and we form the sequence

$$\delta R_j = OA_j - k * \theta_j, \quad j = 1, \ldots, L,$$

where $L$ is the number of the chosen pixels of the actual depicted spiral $\boldsymbol{S^A}$. Next, if $\bar{X}$ is the mean value and $S^2$ is the variance of $\delta R_j$, we once more form the quantity

$$t = \frac{\bar{X}}{S/\sqrt{L}},$$

Figure 4 *The way in which the theoretical model of the linear spiral (the computer-generated red and green lines) best fits to actual parts of smaller-dimension spirals (k = 9.38).*

which follows a Student distribution with $L - 1$ degrees of freedom. Subsequently, applying Criterion 1, we again state and test the hypothesis that the $\delta R_j$ come from a population with $\mu = 0$; that is, we state the hypothesis $H_0 : \mu = 0$, against the hypothesis $H_1 : \mu \neq 0$, with 99.9% confidence or a significance level of $a = 0.001$, for all available spirals. As before, we compare the value of $|t|$ with $t_H$. In fact, $|t|$ ranges from 0.0064 to 3.1, always satisfying $|t| \leq t_H$. Therefore, hypothesis $H_0$ is not rejected for all these spirals (see also Figs 2 and 4).

Note that, in Figure 2, each of the corresponding drawn spirals is best approximated by a single-equation linear spiral. An essentially better approximation can be obtained by dividing the prototype linear spiral into a limited number of stencils and subsequently using them to approximate the drawn spirals, as described in section 4.6.

### *4.6 Approximation of the drawn spirals by linear prototypes*

In this section, we will first give an estimate of the probability that all drawn spirals, whose thematic content is well preserved, have a linear spiral as a prototype. Moreover, the optimal values of the parameters of these prototype spirals will be estimated.

The next step is the determination of the characteristics of these model spirals. In fact, applying the method introduced in section 4.2, we have reached the conclusion that the available spiral parts correspond to at least two classes of prototype linear spirals with different parameters: one class, which we call CLP1, corresponds approximately to the prototype with $\kappa = 1.393$ cm; while the other one, which we call CLP2, is best approximated by at least two prototypes with $\kappa = 0.6263$ cm and $\kappa = 0.2256$ cm. There are at least eight well-preserved actually drawn spirals belonging to class CLP1 and at least 12 well-preserved actually drawn spirals belonging to class CLP2.

We would like to point out that the average distance between the actual and prototype spirals of the first class is between 0.14 and 0.20 cm. If this error is divided by the corresponding spiral radius, then an average percentage error between 1.2% and 1.4% is obtained. Concerning the second prototype spiral class, the average distance is about 0.08 cm, while the corresponding average percentage error is 1.1%.

Subsequently, we would like to point out that extensive archaeological analysis has offered various indications that the artist, or artists, might have used handicraft stencils (templates) in order to draw the wall-paintings (Birtacha and Zacharioudakis 2000). Thus, we have also considered the possibility that the artist drew the spirals by using a number of such stencils. In order to confirm this, we have applied the above-mentioned methodology to achieve a piecewise approximation of the actually depicted spirals. In this way, we have determined six stencils whose combination offers an even closer approximation of the actually drawn spirals. In fact, the average distance between the available actual spirals and the prototype ones is between 0.034 and 0.048 cm, while the average percentage error is between 0.29% and 0.34% and the maximum percentage error is about 0.56%. Moreover, by applying Criterion 2 to these spirals, it follows that the piecewise linear spiral fits them, with probability $P \geq 1 - 10^{-24}$. At this point, we would like to clarify that all reported low errors have been computed on the following basis.

For each spiral image, after the applied image segmentation, edge extraction has been performed and, as a result, the edge of each spiral part is considered to be a connected chain of pixels. The error of approximating the spirals by a corresponding geometrical prototype is estimated by means of the average and maximum distance of each pixel of the edge chain from the corresponding geometric curve. The obtained error precision is limited by the finite resolution of the employed image. In fact, 1 cm of each digital image of an arbitrary considered wall-painting corresponds to at least 59.06 pixels resulting from the resolution of the image and the employed shooting zoom factor. Thus the pixel dimensions of the employed images are 0.169 mm $\times$ 0.169 mm. Therefore, this can be the higher possible precision with which the edge of the specific images can be estimated.

In addition, it can be pointed out that in such small sizes there are ‘uncertainty conditions’, such as the inaccuracy with which the border is obtained, clearly associated with the grain size in the stucco, the probable optical distortions due to the photographic conditions, and so on. Therefore, the exact small value of the distance of the model from the obtained contour may not be an absolute measure of the way in which the stencil approximates the actually drawn object, but it is quite a strong indication that the approximation is really good. The good quality of approximation is also demonstrated in Figure 3 (b).

The reported very good approximation supports the conjecture that the artist constructed a linear spiral first; subsequently, this was divided into probably six stencils, and these were then used to draw the spirals on the wall by successively placing the one stencil after the other (see Fig. 5). In other words, to summarize, the hypotheses that the drawn spirals correspond to involutes of a circle, or to logarithmic spirals or piecewise involutes of a circle, have been rejected. In addition, the hypothesis that the drawn spirals correspond to linear spiral prototypes with one centre cannot be rejected, with a confidence level of 99.9%. If we momentarily adopt this hypothesis, then application of Criterion 2 offers a respectable probability that this may be the case. However, the hypothesis that the artist divided the one central linear spiral prototype into six stencils and used them to draw the corresponding wall-paintings offers a much better approximation, and a probability of being valid that is much closer to 1.

A question that arises is why the artist did not prefer to use the entire linear spiral prototype but, instead, used a set of stencils obtained from a division of the model spiral. A reasonable explanation, besides the fair point that smaller pre-constructed models are easier to carry, seems to be the following. Careful examination of the surface of the wall-paintings reveals the presence of straight-line incisions, which indicate that the artist divided the area of the fresco into a number of almost rectangular sub-regions. In other words, the artist defined a set of guidelines in order to ensure that the wall-painting theme would be as topographically precise

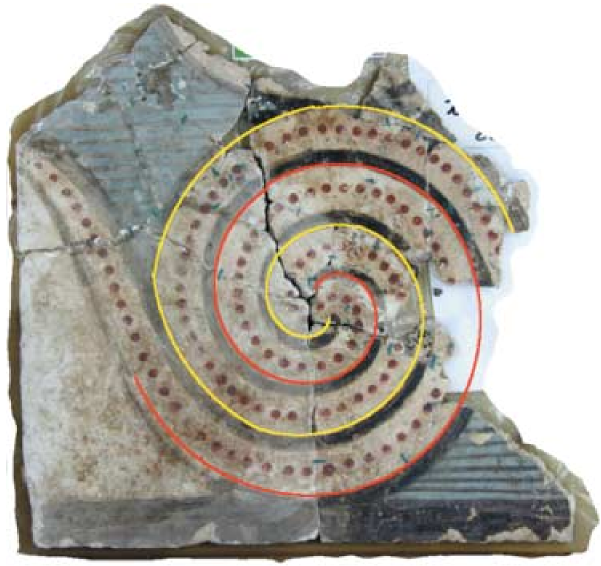

Figure 5 *The excellent way in which the six stencils (the computer-generated red and yellow lines) approximate the corresponding pair of spirals.*

and flawless as possible. Thus, each linear spiral had to fit into a predefined space with the maximum feasible accuracy. The use of a number of stencils rather than a rigid prototype helped the artist to slightly vary the spiral shape to achieve optimal spiral adjustment. The possibility cannot be excluded that an additional reason for the use of stencils is that they helped the artist to convey the desired visual impression.

### *4.7 The hypothesis for the method used for the construction of the linear spiral*

The previous analysis has shown that the actual drawn spiral parts match at least three linear spiral prototypes well. Nevertheless, unless there is a major archaeological find, it will not be possible to determine, with certainty, the exact method that the artist used to construct the prototypes. Therefore, strictly speaking, the possibility cannot be excluded that the artist employed a practical method to draw the spiral parts and that, accidentally, the resulting figures match a linear spiral prototype. All the same, it may be claimed that the above statement is not compatible either with the fact that the artist used at least three different linear spiral prototypes, each one corresponding to an essentially different set of parameters, or to the excellent degree to which the linear spiral prototype approximates the actual drawn ones. We will momentarily, at least, accept the hypothesis that the artist indeed used a geometrical method for drawing the linear spiral. We tend to believe that the following method is, perhaps, the more plausible one for this period. As shown in Figure 6, this method can be described as follows:

(1) Draw a large number of homocentric circles $\Gamma_n$ of common centre O, where two successive circles have a fixed radius difference of, say, $d$.

(2) Divide the $2\pi$ entire angle into $N$ equal angles and draw the corresponding semi-lines $\varepsilon_n$ starting at the same centre O, where, clearly, $\varepsilon_{n-1}$ and $\varepsilon_n$ form an angle $2\pi/N$.

(3) The sequence of points of intersection of $\varepsilon_n$ and $\Gamma_n$ lie on a linear spiral.

The greater the number of lines and circles, the better is the obtained linear spiral approximation.

A possible approach for forming isogonal lines is to start from an easy-to-construct canonical polygon—for example, an equilateral triangle or a square—and then to continually bisect the epicentral angle to obtain a series of canonical polygons, where the *n*th series element has double the number of sides compared to the $(n - 1)$th one.

In what follows, we will take for granted the hypothesis that the artist used the above-mentioned geometrical methods, and we will try to find other possible applications of these methods in the wall-paintings.

## 5 PROBABLE KNOWLEDGE OF DICHOTOMIZING (BISECTING) AN ANGLE AND CONSTRUCTING ISOGONAL LINES

Accomplishment of the above-mentioned linear spiral construction method presupposes knowledge of dividing the 360° ($2\pi$ radians) angle into $N$ equal angles. Following the analysis of the previous section, we have considered the possibility that the artist employed the isogonal straight lines used in the above-mentioned method for drawing other decorative elements too. Thus, for example, consider the black spikes that appear in the second class of spirals (see Fig. 7).

One may state the logical assumption that their position is a result of the artist's attempt to draw them equidistantly. In order to test these assumptions, we have computed the distance between two successive black spikes. A typical sequence of distances for the spikes of Figure 7 is as follows:

| *Cardinal number of successive spikes* | *Distance (cm)* |
|---|---|
| 1–2 | 2.8118 |
| 2–3 | 3.5382 |
| 3–4 | 3.0339 |
| 4–5 | 3.2067 |
| 5–6 | 3.3716 |
| 6–7 | 3.5331 |
| 7–8 | 4.0544 |
| 8–9 | 3.3272 |

After considering all available sequences of black spike distances, we have been unable to see a desire on the part of the artist to draw equidistant black spikes.

In any case, we have considered the possibility that the artist used a stencil of almost equal angles to draw groups of black spikes on the wall. To test this assumption, we have proceeded as follows.

In order to obtain a measure of the goodness of fit of a sequence of angles to a corresponding sequence of equal angles that are epicentral angles of a canonical $N$-gon, we introduce a number of definitions:

(1) We define $\theta a_i$ to be the actual angle between the two semi-lines $\varepsilon_j$ and $\varepsilon_{j+1}$, where $\varepsilon_j$ is the semi-line starting at a certain point $(x_0, y_0)$ and passing through the centre of the $j$th decorative element, $j = 1, 2, \ldots, N_D$, where $N_D$ is the number of decorative elements under consideration.

(2) We define the quantity $\theta A_i = \sum_{n=1}^{i} \theta a_n$.

(3) We define $\theta C\_x = 2\pi/x$, where $x$ is an arbitrary real number.

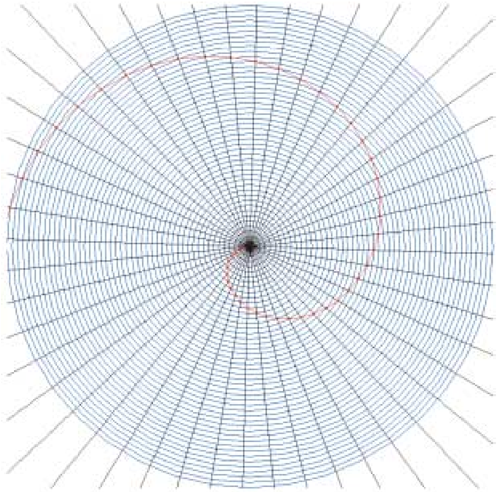

Figure 6 *A geometrical method for generating points lying on a linear spiral.*

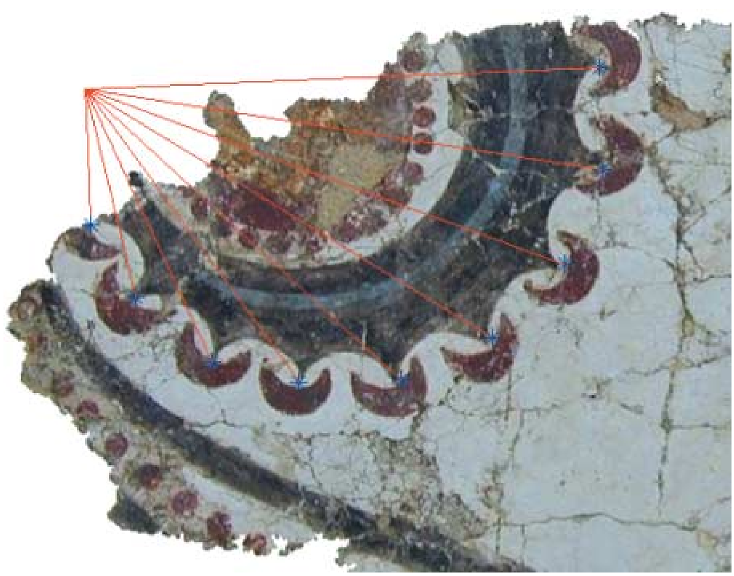

Figure 7 *The black spikes lie on equiangular lines corresponding to the radii of a regular 32-gon.*

(4) We define $\theta C\_xs_i = \theta C\_x0 + (i - 1) * \theta C\_x$, where $\theta C\_x0$ is an arbitrary initial angle.

(5) We define $\Delta_A = \sum_{i=1}^{N_D - 1} \frac{(\theta C\_xs_i - \theta A_i)^2}{\theta C\_xs_i}$.

(6) Then, we define the probability that a point $(x_0, y_0)$ 'sees' all the decorative elements in hand with equal angle $\theta C\_x$ via the relation $P_A = P(x \geq \Delta_A)$.

Next, we want to find out if there is any point O in the wall-painting image plane that forms, with the decorative elements in hand, a number of isogonal lines. In order to do so, we determine

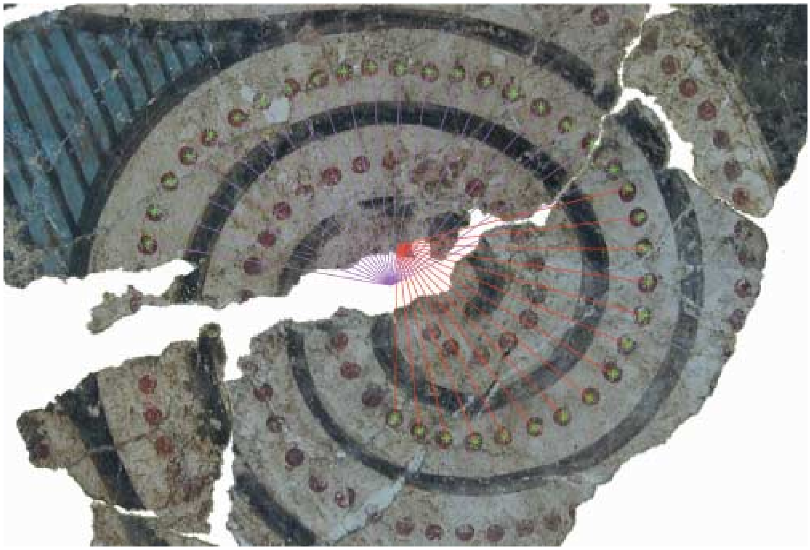

Figure 8 *An optimal approximation of the red dot centres by two equiangular stencils, both of which have all epicentral angles equal to 2π/48. The centres of the stencils lie near to the centres of the linear spirals.*

the point $O^{OPT}$ and a corresponding angle $2\pi/x^{OPT}$ that, amongst all the points of the plane and all real angles, minimize the quantity $\Delta_A$ introduced above. If this minimum $\Delta_A$ is below an acceptable threshold, then we deduce that point $O^{OPT}$ 'sees' all the decorative elements in hand with the same angle $2\pi/x^{OPT}$.

Applying this technique to the black spikes of all available well-preserved CLP2 spirals, we found that there is indeed a point $O^{OPT}$ that 'sees' all of them with an almost fixed angle and, in particular, with the epicentral angle of a canonical 32-gon. The mean discrepancy of $\theta a_i$ from 360°/32 is, on average, less than 0.53°, while the maximum discrepancy is 0.71° (see Fig. 7). We believe that this good approximation supports the hypothesis that the artist used a stencil of equiangular straight lines to draw these decorative elements.

Next, we have looked for analogous decorative elements in the first class of spirals that may have been drawn in an analogous manner, such as the red dots shown in Figure 5. In other words, we have tried to test the hypothesis that the artist drew subgroups of these decorative elements by using such equiangular stencils. Now, the method of testing this hypothesis involves an additional parameter, namely the number of successive red dots considered each time. This third parameter is established by trial and error; in other words, we start with a tentative number of successive red dots, apply the method described above in connection to the black spikes, and continually increase this number, provided that $\Delta_A$ remains below a reasonable threshold.

In this way, we can find a very limited number of 'maximal' subgroups of red dots, together with a corresponding centre $O^{OPT}$ each time, such that $O^{OPT}$ 'sees' the red dot centres of such a subgroup with the epicentral angle of a canonical 48-gon. Two such subgroups and the corresponding centres are shown in Figure 8. The mean discrepancy of the actual epicentral angles $\theta a_i$ from 360°/48 in the first subgroup is on average less than 0.34°, while the maximum discrepancy is 0.92°; and in the second subgroup mean discrepancy is on average less

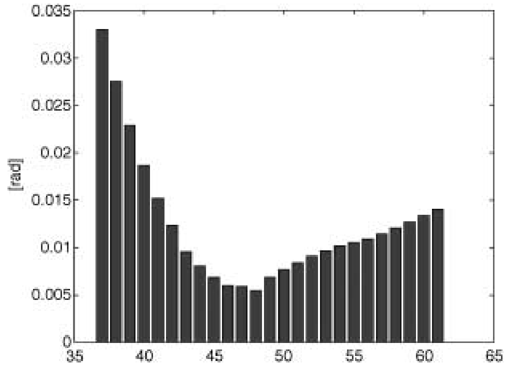


Figure 9 *The average angular distance (in radians) between the optimal equiangular stencil of epicentral angle 2π/N (N = 37–61) and the second subgroup of red dots shown in Figure 8. For example, for N = 40, the equiangular stencil with epicentral angle 2π/40 optimally fits the red dots subgroup with a mean error of 0.0187 rads.*

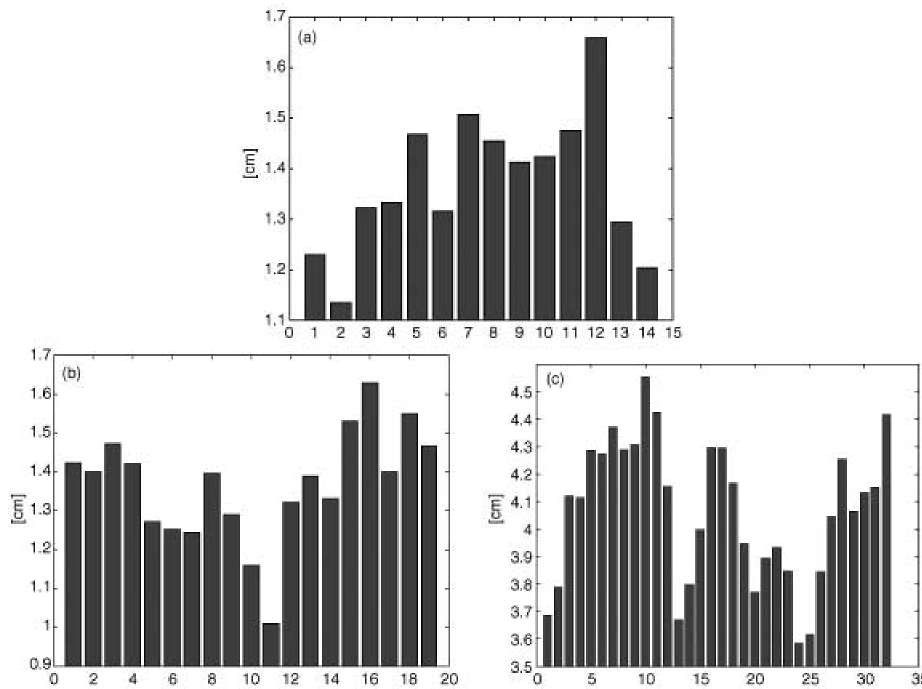


Figure 10 *(a) A plot of the distances between successive red dot centres of the first subgroup shown in Figure 8, corresponding to the first (red) equiangular stencil. (b) A plot of the distances between successive red dot centres of the second subgroup shown in Figure 8, corresponding to the second (magenta) equiangular stencil. (c) A plot of the aggregate distance between any four successive red dot centres in Figure 8. The first bar corresponds to the sum of the distances between the centres of dots 1–4, the second bar to dots 2–5, and so on.*

than 0.31°, while the maximum discrepancy is 0.89°. We would like to point out that employment of a limited number of equiangular stencils in order to draw the red dots is compatible with the assumption that the artist used linear spiral stencils to draw the corresponding figures. Note that we may check whether equally large red dot subsets fit well to equiangular stencils


Figure 11 *The rosette petal separative segments all lie on isogonal semi-lines corresponding to the radii of a canonical 16-gon.*

of an angle corresponding to other canonical polygons; for example, 40- to 47-gon or 49- to 56-gon. In fact, we can repeat the above procedure, each time substituting $x^{OPT}$ with the corresponding number of polygon vertices, and we can calculate the mean angular error. The relative plot for the second subgroup (the magenta equiangular stencil in Fig. 8) is shown in Figure 9, from which it is evident that the lowest error occurs for $x^{OPT} = 48$. Note that for $x^{OPT} \leq 41$ and $x^{OPT} \geq 57$, it is evident by simple inspection that the approximation fails completely. Analogous results also hold for the first red dots subgroup. We would like to emphasize that the regular 48-gon can be constructed by means of a ruler and a pair of compasses, while the other canonical polygons entering the plots of Figure 9 cannot. In fact, the canonical 48-gon can be constructed by first bisecting the angle of a canonical hexagon, then bisecting the angle of the obtained regular 12-gon and eventually dichotomizing the epicentral angle of the resulting regular 24-gon. Thus, we emphasize that although average angular errors in the case of regular canonical 48-gons, 49-gons and 50-gons are quite close in at least one of the considered red dot subgroups, the 49-gon or 50-gon, and so on, stencils are excluded for reasons of constructability.

One may still make the plausible assumption that the placement of these red dots is a result of the artist's attempt to draw them equidistantly. The distance between any two successive red dot centres has been estimated both for the entire set of red dots as well as for the specific subsets. Moreover, we have computed the distance between $n$ successive dots, $n = 2, 3, 4, 5, 6$. The corresponding results for $n = 1$ and $n = 4$ are shown in Figure 10.

Considering all of the above results, we feel that it is probable that the specific subgroups of red dots have been drawn by means of an equiangular stencil, where each angle is equal to the epicentral angle of a canonical 48-gon. Note that we have found such red dot subgroups for all available CLP1 spirals.

Finally, we have determined other decorative elements, not necessarily directly connected to spirals, that support the hypothesis that the artist knew how to construct epicentral angles of regular 16-gons, 32-gons and 48-gons: see, for example, the rosette in Figure 11.

## 6 CONCLUSIONS

In this paper, a very important wall-painting, initially decorating the internal walls of the third floor of the 'Xeste 3' edifice excavated at Akrotiri, Thera, has been considered. Particular emphasis has been given to the study of the geometrical patterns appearing in this wall-painting, which are drawn with noticeably steady lines and are regularly distributed on the painted surface of the wall. In fact, in order to study these figures, an original methodology has been developed and introduced here. The application of this new approach has demonstrated that the spirals depicted on the specific wall-painting correspond, with exceptional accuracy, to linear spirals. In addition, it has been shown that there are many sets of decorative elements placed, with impressive precision, along the radii of various canonical polygons. The hypothesis that these geometrical motifs were drawn on the wall with the use of handicraft stencils, probably made via geometrical methods, has been stated and supported.

It has been pointed out that the first- and second-floor internal murals of 'Xeste 3' are decorated with a huge amount of pictorial and narrative scenes. On the contrary, the wall-painting first considered in this paper seems to have been made according to a strict iconographical programme. These characteristics of the 'Xeste 3' third-floor wall-paintings favour a distinct—yet unknown—use of the corresponding space, which we have attempted to elucidate with our multidisciplinary approach to the wall-paintings.

## REFERENCES


Birtacha, K., and Zacharioudakis, M., 2000, Stereotypes in Thera wall paintings: models and patterns in the procedure of painting, in *Proceedings of the First International Symposium 'The Wall Paintings of Thera', Athens, 2000* (ed. S. Sherrat), 159–72.

Doumas, C., 1990, The elements at Akrotiri, in *Thera and the Aegean world III* (ed. D. A. Hardy), 24–30, The Thera Foundation, London.

Doumas, C., 1992, *The wall-paintings of Thera*, 14–15, The Thera Foundation, Athens.

Heath, T., 1981 [1921], *A history of Greek mathematics*, Dover Publications, New York; first published in 1921 by the Clarendon Press, Oxford.

Papaodysseus, C., Panagopoulos,T., Exarhos, M., Triantafillou, C., Fragoulis, D., and Doumas, C., 2002, Contour-shape based reconstruction of fragmented, 1650 BC wall paintings, *IEEE Transactions on Signal Processing*, **50**(6), 1277–88.

Pearson, E., D'Agostino, R., and Bowman, K., 1977, Tests for departure from normality: comparison of powers, *Biometrika*, **64**, 231–46.

Robson, E., 1999, *Mesopotamian mathematics, 2100–1600 BC*, 144–5, Clarendon Press, Oxford/Dover Publications, New York.

Spandagos, E., Spandagou, R., and Travlou, D., 2000, *The mathematicians of ancient Greece, Aethra (Οι Μαθηματικοί της Αρχαίας Ελλάδος)*, 189–91, Aethra Publications, Athens.